Modelling amplification effects of cascading failures of landside dams

Mingfu Guan
Assistant Professor, Department of Civil Engineering, the University of Hong Kong, Hong Kong SAR
Corresponding e-mail: mfguan@hku.hk

Qingyuan Yang
Department of Civil Engineering, the University of Hong Kong, Hong Kong SAR
Changjiang River Scientific Research Institute, Wuhan, China

ABSTRACT: This study evaluates the formation and development of rapid sediment-charged floods due to cascading failure of landslide dams through detailed hydro-morphodynamic modelling. The model used is based on shallow water theory and it has been successful in predicting the flow and morphological process during sudden dam-break, as well as full and partial dyke-breach. Various experimental-scale scenarios are modelled, including: (1) failure of a single full dam in a sloping channel, (2) failure of two dams in a sloping channel, (3) failure of multiple landslide dams (four) in a sloping channel. For each scenario, different failure modes (sudden/gradual) and bed boundary (fixed /mobile) are assumed and simulated. The study systematically explores the tempo-spatial evolution of landslide-induced floods (discharge, flow velocity, and flow concentration) and geomorphic properties along the sloping channel. The effects of in-channel erosion and flow-driven sediment from dams on the development of flood process are investigated. The results improve the understanding of the formation and development mechanism of flash floods due to cascading landslide dam failures. The findings are beneficial for downstream flood risk assessment and developing control strategies for landslide-induced floods.

1 INTRODUCTION

Landslide dams are commonly formed in a river valley of mountainous areas due to heavy rainfall or earthquake, which can be a complete or partial blockage (Ermini and Casagli, 2003; Zhou et al., 2016). Different from conventional man-made dams, landslide dams typically comprise unconsolidated and poorly sorted material, and are vulnerable to failure and breaching in short period due to overtopping or seepage. Numerous field evidence has indicated the various risks of landslide dam failures, e.g. the Wenchuan earthquake-induced landslide floods in 2008, and the recent Nepal earthquake-induced floods. Studies have indicated the over 90% landslide dam failure are driven by flow overtopping and over 80% occurred within half-year of their formation (Schuster et al., 1986; Costa and Schuster, 1988). For those small sediment blockage in a river valley, their failures frequently occur during high intense rainfalls, which will induce a large flash flood with high-concentrated sediment downstream in a short period, and the magnitude is likely to be amplified along the flow direction due to the inclusion of a large amount of sediment. This can result in significant and sudden debris flow or flood risk downstream for human life and property, such as 2010 debris flow in Zhouqu, China. Cascade failures of a series of landslide dams in a gully have been considered to be a primary reason for the enlargement of high sediment-laden flood. In general, cascading landslide dams can be formed along the sloping channel due to the randomness and unpredictability of landslides, which complexes the hydraulics of landslide dam failures. The failure process of a single natural dam and subsequent floods has widely studied (Guan et al., 2014; Cao et al, 2011; Walder et al., 2015; Bento et al, 2017; Di Cristo et al., 2018). However, the dynamic failure process of cascading landslide dams more than 3 has been poorly understood.

Field and experimental studies on cascade failures of small natural dams have been conducted to understand the physical processes (Chen et al., 2014; Zhou et al., 2015). Yet the suddenness of real-world events and inadequate monitored data of experiments limit the in-depth understanding of the whole physical processes of the cascade failures, e.g. temporal and spatial dynamics under various scenarios with different dam properties. Recent developments of reliable

numerical models have provided supports to develop a greater understanding of hydraulics for the evolution of sediment-laden flows. Therefore, build upon the hydro-morphodynamic model we have developed (Guan et al., 2014), this study reproduces the physical processes of a prototype of debris flow evolution due to a series of sediment blockage in a river valley. This study designs various blockage scenarios and simulates the full hydraulic and morphological dynamic process for each, so as to better understanding of hydraulics of a cascade failure of natural dams from the numerical viewpoint. The hydro-morphodynamic model is a coupled model of 2D shallow water model and a bedload dominant sheet flow model with an inclusion of bed slope avalanching.

2 COMPUTATIONAL MODEL

A combined model of sheet flow and suspended load is applied to simulate it. The computational model is briefly described as:

2.1 Hydro-morphodynamic model

The hydro-morphodynamic model is governed by 2D shallow water equations and non-equilibrium sediment transport model that is widely used (Cao et al, 2004; Wu, 2007; Canelas et al., 2013; Guan et al. 2014). As in mountainous area, bedload is generally dominate transport mode, the sheet flow model dominated by bedload and partially suspended load is used. More details about the model and numerical algorithm can be found in Guan et al. (2014). Governing equations is expressed by:

$$\frac{\partial \eta}{\partial t}+\frac{\partial hu}{\partial x}+\frac{\partial hv}{\partial y}=0 \tag{1}$$

$$\frac{\partial hu}{\partial t}+\frac{\partial}{\partial x}\left(hu^2+\frac{1}{2}gh^2\right)+\frac{\partial}{\partial y}huv=gh\left(S_{ox}-S_{fx}\right)+\frac{\Delta\rho u}{\rho}\frac{\partial z_b}{\partial t}\left(\frac{1-p}{\beta}-C\right)-\frac{\Delta\rho gh^2}{2\rho}\frac{\partial C}{\partial x} \tag{2a}$$

$$\frac{\partial hu}{\partial t}+\frac{\partial}{\partial x}huv+\frac{\partial}{\partial y}\left(hv^2+\frac{1}{2}gh^2\right)=gh\left(S_{oy}-S_{fy}\right)+\frac{\Delta\rho v}{\rho}\frac{\partial z_b}{\partial t}\left(\frac{1-p}{\beta}-C\right)-\frac{\Delta\rho gh^2}{2\rho}\frac{\partial C}{\partial y} \tag{2b}$$

$$\frac{\partial hC}{\partial t}+\frac{\partial huC}{\beta\partial x}+\frac{\partial hvC}{\beta\partial y}=-\frac{(q_b-q_{b*})}{\beta L} \tag{3}$$

where h = flow depth (m), z_b = bed elevation (m), $\eta = h + z_b$ denotes the water surface elevation which includes both changes of the water depth and bed elevation varying with the time t, u and v = the depth-averaged flow velocity components in the two Cartesian directions (m/s), g = acceleration due to gravity (m/s^2), p = sediment porosity (dimensionless), C = volumetric sediment concentration (dimensionless), $\Delta\rho = \rho_s - \rho_w$ = the difference of sediment density (ρ_s) and water density (ρ_w) (m^3/s), $\rho = \rho_w(1\text{-}C)+\rho_s C$ = density of flow-sediment mixture (m^3/s), S_{ox}, S_{oy} are the bed slopes in x and y direction; S_{fx}, S_{fy} are the frictional slopes in x and y direction calculated based on manning's roughness n; L=non-equilibrium adaptation coefficient of sediment transport (m) determined by:

$$L=\frac{h\sqrt{u^2+v^2}}{\gamma\omega} \text{ with } \gamma=\min\left(\beta\frac{h}{h_b},\frac{1-p}{C}\right) \tag{4}$$

in which, $h_b = 9\theta d_{50}$ is the thickness of sheet flow layer (Pugh and Wilson 1999, Ferreira et al, 2009), θ is the dimensionless bed shear stress. Flow-to-sediment velocity ratio β is calculated by:

$$\beta=\begin{cases}\dfrac{u}{u_b}=\dfrac{u}{u_*}\dfrac{\sqrt{\theta_c}}{1.1(\theta/\theta_c)^{0.17}[1-\exp(-5\theta/\theta_c)]} & \theta/\theta_c<20\\ 1 & \theta/\theta_c\geq 20\end{cases} \tag{5}$$

where $u_*=\sqrt{\theta(\rho_s/\rho_w-1)gd}$ is the shear velocity, d is the median sediment diameter; θ_c is the critical dimensionless bed shear stress for sediment motion incipient calculated by the formula proposed by Soulsby (Soulsby 1997). The Meyer-Peter & Müller equation (*MPM*) (Meyer-Peter and Müller 1948) has been recalibrated by Wong and Parker (2006), and below updated formula is used to calculate bedload-dominant transport rate:

$$q_{b*} = 4.93(\theta - 0.047)^{1.6}\sqrt{(\rho_s/\rho_w - 1)gd^3} \quad (6)$$

The morphological evolution is determined by the difference of real sediment transport rate and sediment transport capacity that is calculated per grid cell at each time step.

$$\frac{\partial z_b}{\partial t} = \frac{1}{1-p}\frac{(q_b - q_{b*})}{L} \quad (7)$$

where $q_b = hC\sqrt{u^2 + v^2}$ is the real sediment transport rate.

Eqs.(1)-(3) constitute a shallow water non-linear system which are numerically solved by a well-balanced Godunov-type shock capturing numerical algorithm based on Cartesian coordinates. The numerical model has been validated by a series of laboratory experiments as described in Guan et al. (2014), such as dam-break flow over movable bed with fixed width and sudden enlarged width, as well as dam erosion due to full and partial flow overtopping. The validation justifies the model's capability of reasonably reproducing the hydro-morphodynamic processes of natural dam/dyke/embankment erosion. Although it has been reported that closure parameters such as manning's roughness, choice of sediment transport formula and velocity ratio can sensitively affect bed changes driven by flows (Wu, 2007; Canelas et al., 2013), qualitative assessments for below scenarios are still valuable and results still provide insights into amplification effects of a cascade of landside dams failures. Parameters sensitives are not taken account for the time being.

2.2 Model scenarios

An experiment regarding the cascade landslide dam failures has been conducted by Chen et al., (2014). The limitations of measurement and experimental conditions lead to a lack of datasets for comprehensive hydraulic analysis. Therefore, the modelling scenarios here will be based on the experimental conditions by Chen et al., (2014). The experimental flume is composed of an upstream reservoir with a horizontal bottom of 4.6m long, 0.7m wide and 1.4m high, and a downstream channel with a slope of 12° of 47.3 m long, 0.7 m wide and 1.4 m high. The initial water volume in the reservoir is 1.45L and water depth is 0.45m. A sluice gate was used to control the water depth of the upstream reservoir. For all below designed scenarios, the gate is suddenly lifted to induce a first dam-break flash flood. Then the floodwater is flowing over a series of full blockage natural dams that are located in downstream channels at regular intervals. Dam1 (D1) size is defined as 1.5m in bottom length and 0.6m in height, and both waterfront and waterback slope is the same. Sediment particle parameter is about 0.002 m. The setup for each scenario is described in Table 1 and illustrated in Figure 1.

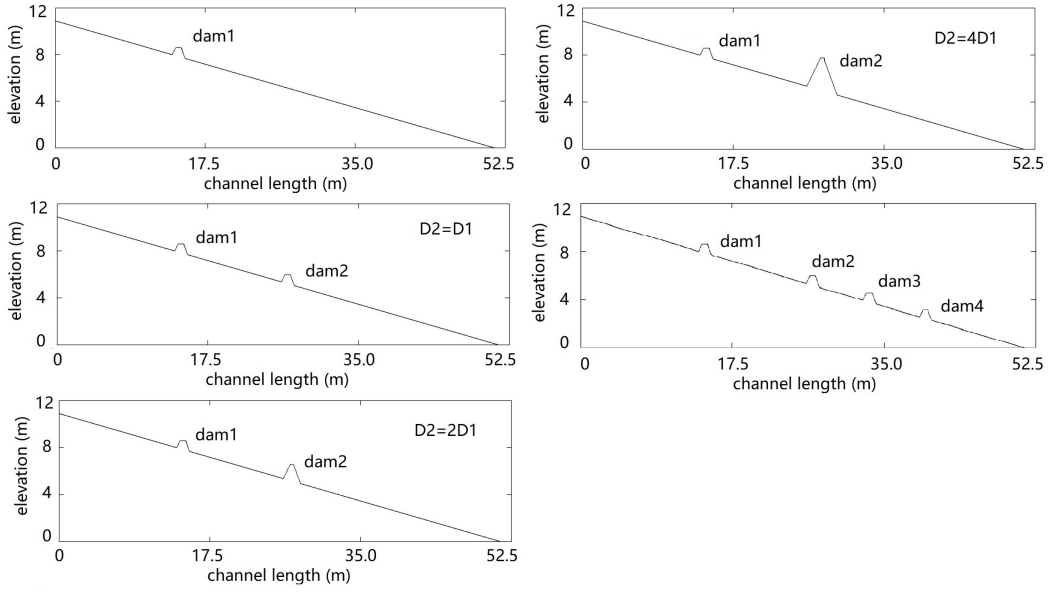

Figure 1. Modelling scenarios

Table 1. Modelling scenarios

scenarios	Dam size					
dams	1 dam	2dams:D2=D1	2dams:D2=2D1	2dams:D_2=4D_1	4 dams	distant to gate (m)
D1	D1	D1	D1	D1	D1	9.74
D2	x	D1	2D1	4D1	D1	22.12
D3	x	x	x	x	D1	28.62
D4	x	x	x	x	D1	35.14

3. RESULTS

3.1 Single landslide dam in the channel

As defined in Figure1 and Table 1, this scenario includes one single landslide dam. First, we perform two simulations in order to justify the effects of sediment transport of channel bed on flow hydraulics: (1) the dam is movable but downstream channel are not movable, (2) both dam and channel are erodible. Flow discharge and velocity are generally key parameters to evaluate the magnitude of a flow event. Therefore, we plot the peak flow discharge and peak velocity along with the channel in Figure 2. Results indicate that both flow discharge and velocity have the same peak value in front of the dam, because that area is fixed bed for both cases. However, it is shown that the peak discharge in downstream channel is remarkably increasing after the flow scours the landslide dam and induces erosion in movable channel area; the peak discharge reaches the maximum value at the downstream boundary of erodible area and fixed area. The bed change shown in Figure 2 explains the potential main causes. The flow induces more and more amount of sediment along with the channel into the water flow which leads to the flow become mixture of water and sediment, say debris flow, and the density is higher compared with the case with only dam is erodible. Therefore, the bulk effects that is emphasized by many research (Guan et al., 2015, 2016) cause an increase of peak discharge along with the channel. It is seen that the sedimentation at downstream channel results in a decrease of peak discharge from the maximum value. In contrast, peak flow velocity is slightly reduced due to more sediment is in motion, which can be explained by the lag effects of sediments within the flow.

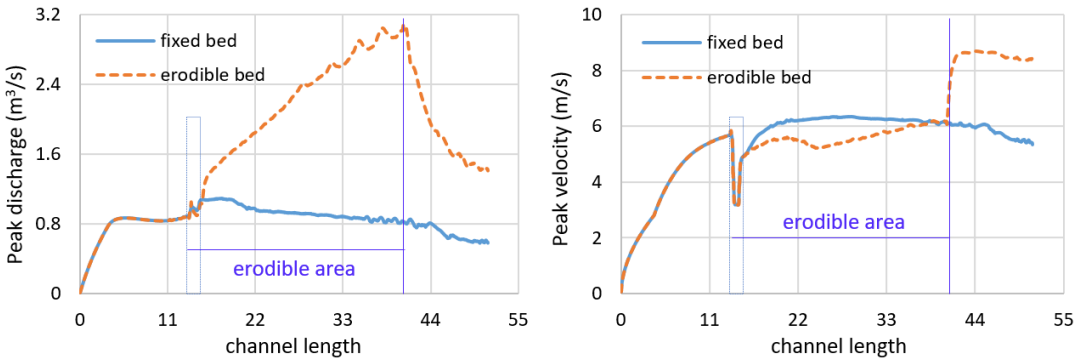

Figure 2. Simulated peak discharge (left) and peak velocity (right) along the channel

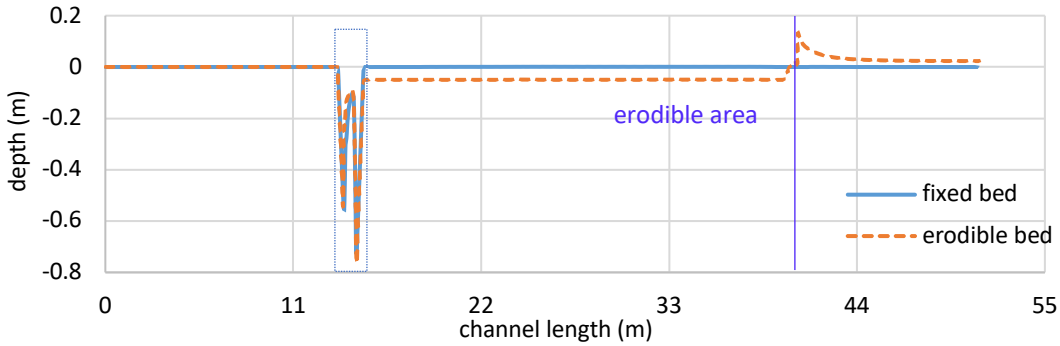

Figure 3. Simulated bed change for the cases with fixed bed and erodible bed at channel downstream

3.2 Two landslide dams in the channel

In order to explore the hydraulics in presence of multiple dams, we first apply the model to simulate the evolution of sediment-laden flow over the channel with two landslide dams. It is assumed that only landslide dams are erodible and the channel bed is fixed so as to specifically verity the hydraulic effects from the dams rather than channel bed. As indicated in section 2.2, the second dam with three different sizes is defined. Still the peak flow discharge and peak flow velocity is plotted in Figure 4. It shows that hydraulics in upstream of dam2 are the same for all three cases because the same size of dam1 and upstream conditions, which is also consistent with single dam scenario shown above. From the velocity profile, we can see that the water is first slowed down when it reach dam1. After the dam is failed both peak flow discharge and velocity have a sharp increase. If there is a second dam with similar size of dam1 located downstream, it is shown that the flow is again slowed down first, and then a burst of sediment-laden flow propagates downstream after dam2 failure. And again the peak flow discharge is further increased compared with the peak after dam1 failure and with the peak flow at this location for single dam scenario (shown in Figure 4 left). However, it is shown that both peak flow discharge and velocity is reduced if dam2 has a bigger size of about 2 dam1 compared with the results of the scenario with single dam. This phenomenon is further amplified if dam2 has an enough size that can fully block the upstream flows (see the results of D2=4D1). Figure 5 illustrates the dam failure process of dam1 and dam2 with the three sizes. The erosion of dam1 is slightly more severe with dam2 (D2=D1), because of the increase of peak flow discharge and velocity due to the bulk effects of sediment. The increase in dam2 size (D2=2D1) raise the blockage capability of dam2, so majority of sediment-laden flow is tracked in front of the dam and sediments are precipitated out from the sediment-laden flows. Part of flow overtopping still cause erosion on the back of dam2. When dam2 has a size of four times of dam1, it is clearly shown that all upstream sediment-laden flows after dam1 failure are stored and sediments are deposited in front of dam2 which becomes a natural barrier lake. However, this increase the potential flood risks at the downstream if the natural dam2 cannot be treated effectively, because if any incoming upstream flows, they will ultimately raise the water level in the lake until flow overtopping and dam failure. As reported by a number of studies (Guan et al., 2015), the failure of barrier lake is fatal.

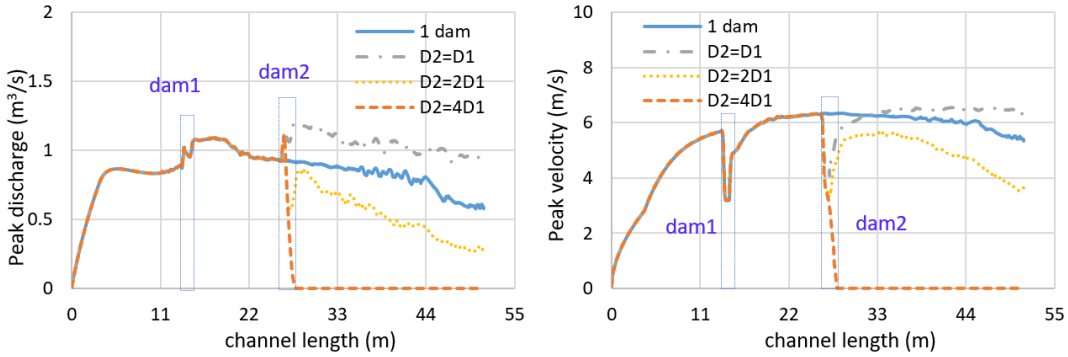

Figure 4. Simulated peak discharge (left) and peak velocity (right) along the channel

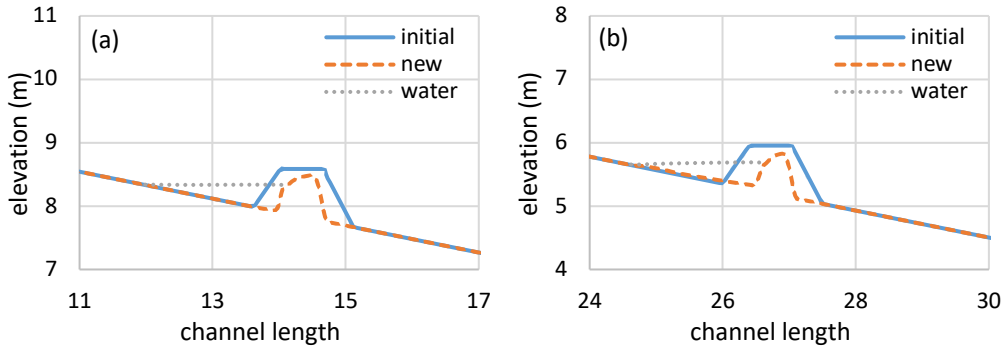

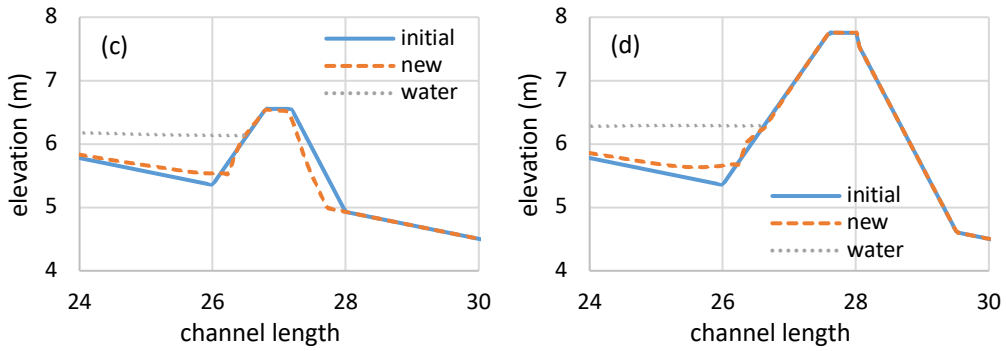

Figure 5. Initial dam and simulated eroded dam for (a) dam 1, (b) dam2 with D2=D1, (c) dam2 with D2=2D1, and (d) dam 2 with D2=4D1

3.3 Four landslide dams in the channel

As discussed above, the bulk effects of sediment within waterflow lead to an increase of flow discharge at downstream. In reality, a valley can generally be blocked with a series of landslide dams. To justify the dynamic process, we then reproduce the experimental scenario with four small dams with a same size described in Chen et al. (2014), and results are plotted in Figure 6. It indicates that none of the dams in the channel block the flow movement, but the dam amplifies the magnitude of the flow. When the flow reaches each dam, peak velocity is only temporarily reduced. Any dam failure must lead to an increase of peak flow discharge. From the upstream to downstream dam4, the peak flow discharge is increased by 80%, the peak velocity is also increased to some extent. The erosion profile of each dam shown in Figure 7 shows that sediments eroded from each dam are replenished into the mixture of sediment and water (debris flow). It is expected that more landslide dams in the channel will that cannot stop the flow will lead to much higher peak downstream discharge. Unless the downstream is enough big to form a barrier lake, the hazard risk downstream will be much higher. As emphasized above, the formation of barrier lake may help to protect one-off sediment-laden floods and allow more time for downstream response. However, this exposes downstream area into a higher risk if there are continuous incoming flows at the upstream, e.g. intense rainfall induces another flash flood.

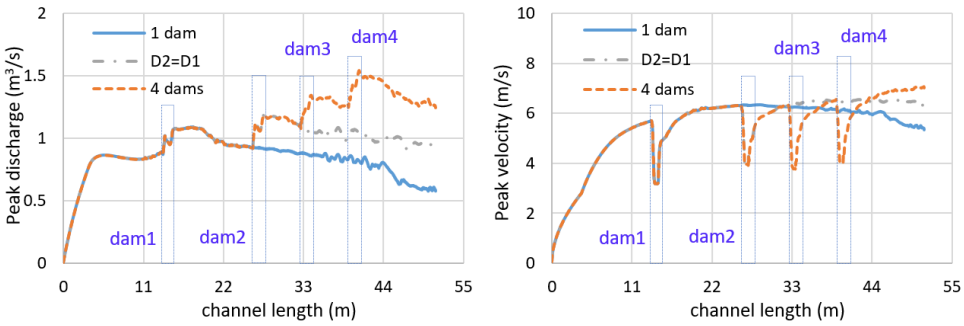

Figure 6. Simulated peak discharge (left) and peak velocity (right) along the channel

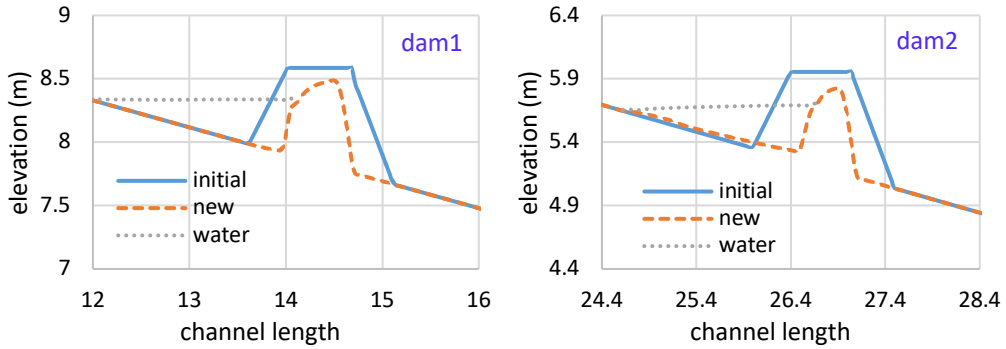

dam3

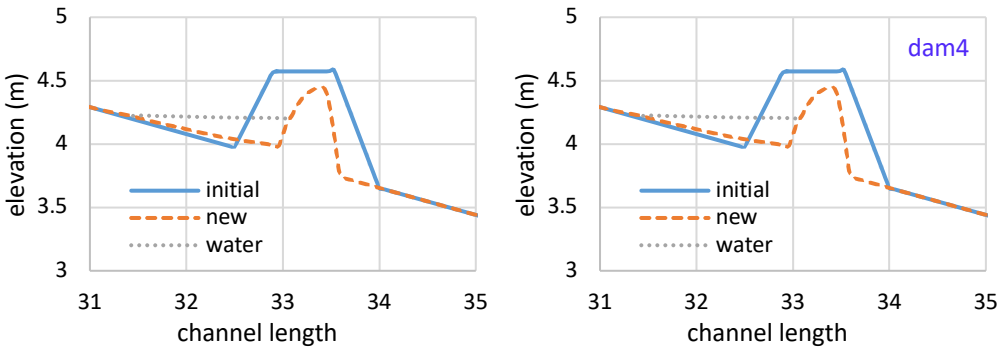

Figure 7. Initial dam and simulated eroded dam for the four dams

4. CONCLUSION

This study systematically investigates tempo-spatial dynamic processes of a series of landslide dam failures based on numerical simulations of various scenarios, including: (1) failure of a single full dam in a sloping channel, (2) failure of two dams in a sloping channel, (3) failure of four landslide dams in a sloping channel. Results indicate that the flow can be amplified by the failure of downstream landslide dams because of the bulk effects of sediments, and the more sediments are induced by the flow, the higher peak flow discharge will be caused. Also, the peak discharge at downstream is affected by the number of small landslide dams in the channel. Any dam failure must lead to a sharp increase of peak flow discharge The downstream landslide dam with big size can prevent the propagation of sediment-laden flow, however, this leads to a formation of barrier lake, which also poses high risk to downstream particularly in case of further incoming discharge at upstream. Results numerically verify the formation mechanism of rapid sediment-laden flows and improve the understanding of amplification of sediment-laden flows in propagation due to inclusion of sediments. The findings are beneficial for downstream flood risk assessment and developing control strategies for landslide-induced floods.

5. ACKNOWLEDGEMENTS

The authors' work is supported by Seed Funding of the University of Hong Kong (No. 201812159002) and National Natural Science Foundation of China Youth Grant (No. 51909227).

6. REFERENCES

Bento, A. M., Amaral, S., Viseu, T., Cardoso, R., & Ferreira, R. M. L. (2017). Direct Estimate of the Breach Hydrograph of an Overtopped Earth Dam. Journal of Hydraulic Engineering, 143(6), 06017004.

Canelas, R., Murillo, J., & Ferreira, R. M. L. (2013). Two-dimensional depth-averaged modelling of dam-break flows over mobile beds. Journal of Hydraulic Research, 51(4), 392–407.

Cao, Z., Pender, G., Wallis, S. and Carling, P., 2004. Computational dam-break hydraulics over erodible sediment bed. *Journal of hydraulic engineering*, *130*(7), pp.689-703.

Cao, Z., Yue, Z. and Pender, G., 2011. Landslide dam failure and flood hydraulics. Part I: experimental investigation. *Natural hazards*, *59*(2), pp.1003-1019.

Chen HY, Cui, P., Zhou, G.D., Zhu, X.H. and Tang, J.B., 2014. Experimental study of debris flow caused by domino failures of landslide dams. *International Journal of Sediment Research*, *29*(3), pp.414-422.

Costa, J.E. and Schuster, R.L., 1988. The formation and failure of natural dams. Geological society of America bulletin, 100(7), pp.1054-1068.

Di Cristo, C., Evangelista, S., Greco, M., Iervolino, M., Leopardi, A. and Vacca, A., 2018. Dam-break waves over an erodible embankment: experiments and simulations. *Journal of Hydraulic Research*, *56*(2), pp.196-210.

Ermini L, Casagli N. Prediction of the behaviour of landslide dams using a geomorphological dimensionless index. Earth Surface Processes and Landforms: The Journal of the British Geomorphological Research Group. 2003 Jan;28(1):31-47.

Ferreira, R.M.L.; Franca, M.J.; Leal, J.G.A.B. & Cardoso, A.H. (2009) Mathematical modelling of shallow flows: Closure models drawn from grain-scale mechanics of sediment transport and flow hydrodynamics. Canadian Journal of Civil Engineering, 36(10): 1605-1621. DOI:10.1139/L09-033

Guan, M., Wright, N.G. and Sleigh, P.A., 2014. 2D process-based morphodynamic model for flooding by noncohesive dyke breach. *Journal of Hydraulic Engineering*, *140*(7), p.04014022.

Guan, M., Wright, N.G., Sleigh, P.A. and Carrivick, J.L., 2015. Assessment of hydro-morphodynamic modelling and geomorphological impacts of a sediment-charged jökulhlaup, at Sólheimajökull, Iceland. *Journal of Hydrology*, *530*, pp.336-349.

Guan, M., Carrivick, J.L., Wright, N.G., Sleigh, P.A. and Staines, K.E., 2016. Quantifying the combined effects of multiple extreme floods on river channel geometry and on flood hazards. Journal of Hydrology, 538, pp.256-268.

Morris, M. W., Hassan, M., and Vaskinn, K. A. (2007). "Breach formation: Field test and laboratory experiments." Journal of Hydraulic Research, 45, 9-17.

Pugh, F. J., and Wilson, K. C. (1999). "Velocity and concentration distributions in sheet flow above plane beds." 502 Journal of Hydraulic Engineering, 125(2), 117-125.

Schuster, R.L., 1986. Landslide dams: processes, risk, and mitigation. ASCE.

Walder, J. S., Iverson, R. M., Godt, J. W., Logan, M., & Solovitz, S. A. (2015). Controls on the breach geometry and flood hydrograph during overtopping of non-cohesive earthen dams. Water Resources Research, 51(8), 6701–6724.

Wong, M. and Parker, G., 2006. Reanalysis and correction of bed-load relation of Meyer-Peter and Müller using their own database. Journal of Hydraulic Engineering, 132(11), pp.1159-1168.

Wu, W., 2007. Computational river dynamics. CRC Press.

Zhou, G.G., Cui, P., Zhu, X., Tang, J., Chen, H. and Sun, Q., 2015. A preliminary study of the failure mechanisms of cascading landslide dams. International Journal of Sediment Research, 30(3), pp.223-234.